

## High spatial resolution subsurface microscopy

S. B. Ippolito,<sup>a)</sup> B. B. Goldberg, and M. S. Ünlü

*Departments of Physics and Electrical and Computer Engineering and the Photonics Center, Boston University, 8 Saint Mary's Street, Boston, Massachusetts 02215*

(Received 26 January 2001; accepted for publication 7 May 2001)

We present a high-spatial-resolution subsurface microscopy technique that significantly increases the numerical aperture of a microscope without introducing an additional spherical aberration. Consequently, the diffraction-limited spatial resolution is improved beyond the limit of standard subsurface microscopy. By realizing a numerical aperture of 3.4, we experimentally demonstrate a lateral spatial resolution of better than  $0.23 \mu\text{m}$  in subsurface inspection of Si integrated circuits at near infrared wavelengths. © 2001 American Institute of Physics. [DOI: 10.1063/1.1381574]

Diffraction limits standard optical microscopy to a spatial resolution of about half the wavelength of light. Reducing the wavelength or increasing the collected solid angle can improve the spatial resolution of surface microscopy. This has been achieved both with oil immersion and solid immersion lens<sup>1-4</sup> microscopy techniques, which reduce the wavelength by immersing the object space in a material with a high refractive index. However, in subsurface microscopy the only method to improve the spatial resolution is to increase the collected solid angle. Most standard beam profiles have a full-width-at-half-maximum (FWHM) or lateral spatial resolution limit near  $\lambda_0/(2 \times \text{NA})$  where  $\lambda_0$  is the free space wavelength (also termed the Houston criterion). Therefore, to improve the lateral spatial resolution limit, the numerical aperture (NA) must be increased. The NA is  $n \sin \theta$ , where  $n$  is the refractive index in the object space and  $\theta$  is the half-angle subtended. The larger refractive index ( $n$ ) in the object space in standard subsurface microscopy of planar samples does not increase the NA because of refraction at the planar boundary. This refraction also imparts a spherical aberration, which increases monotonically with NA, reducing the spatial resolution in the absence of correction. The subsurface microscopy technique we describe significantly increases the NA without introducing an additional spherical aberration and thus improves the spatial resolution.

We chose the application area of Si inspection to demonstrate the spatial resolution improvement of the subsurface microscopy technique. Current Si integrated circuit (IC) technology includes many opaque metal layers and structures above semiconductor devices, thereby hindering topside inspection of buried devices in their final state. Therefore, inspection through the backside or substrate of a Si IC is often preferred.<sup>5</sup> However, optical absorption in Si limits inspection through the substrate to  $\lambda_0 \geq 1 \mu\text{m}$ , yielding a theoretical lateral spatial resolution limit for standard subsurface microscopy of  $0.5 \mu\text{m}$ . Typical lateral spatial resolution values for commercial systems are about  $1 \mu\text{m}$ . Meanwhile, modern Si IC technology has reached process size scales of  $0.13 \mu\text{m}$ , clearly beyond the capability of standard subsurface microscopy. The large refractive index of Si ( $n = 3.6$  at  $\lambda_0 = 1 \mu\text{m}$ ) offers the potential for significant improvement in spatial

resolution. The numerical aperture increasing lens (NAIL) subsurface microscopy technique described below improves the theoretical lateral spatial resolution limit to  $0.14 \mu\text{m}$ . We experimentally demonstrate a lateral spatial resolution of better than  $0.23 \mu\text{m}$ , which to the best of our knowledge is a lateral spatial resolution record for backside inspection of a Si IC.

The NAIL is placed on the surface of a sample as illustrated in Fig. 1. Ideally the NAIL is made of the same material as the sample, in this case Si, both polished to allow intimate contact to avoid reflections at the planar interface. The convex surface of the NAIL is spherical with a radius of curvature of  $R$ . Light passes through the sample and NAIL from an object space in the sample at a vertical depth of  $X$ . To increase the NA without introducing an additional spherical aberration, the vertical thickness of the lens is selected to be  $D = R(1 + 1/n) - X$ . In this case the object space coincides with the aplanatic points of the NAIL's spherical surface, which satisfies the sine-condition yielding spherical aberration free or stigmatic imaging.<sup>6</sup> This configuration is similar to that of a solid immersion lens<sup>2,3</sup> where the aplanatic points defined by the spherical surface coincide with an object space on the planar surface of the lens. The NAIL effectively transforms the planar sample into an integrated solid immersion lens.

Addition of the NAIL to a standard microscope increases the NA by a factor of  $n^2$ , up to  $\text{NA} = n$ . In Si at  $\lambda_0 = 1 \mu\text{m}$ , the NA is increased by a factor of 13, up to  $\text{NA} = 3.6$ , corresponding to a lateral spatial resolution limit of

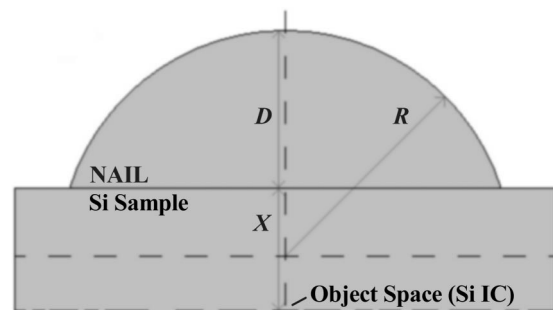


FIG. 1. Schematic representation of NAIL and sample parameters where  $D$  is the vertical thickness of the NAIL,  $R$  is the radius of curvature of the NAIL's spherical surface, and  $X$  is the vertical depth of the sample.

<sup>a)</sup>Electronic mail: ippolito@bu.edu

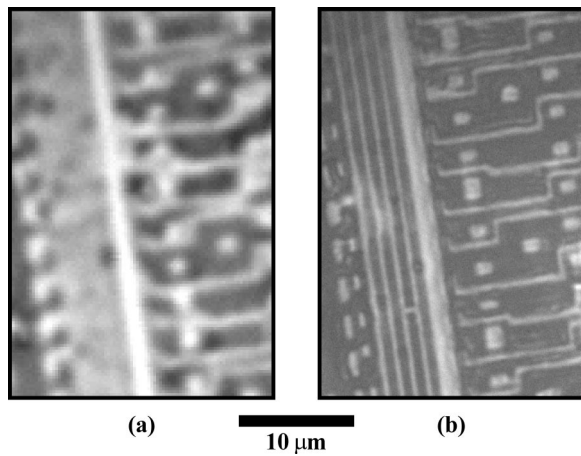


FIG. 2. Images taken by a Hamamatsu  $\mu$ AMOS-200, IC Failure Analysis System, using its (a) 100 $\times$  objective having NA=0.5 and (b) 20 $\times$  objective with a NAIL having NA=3.3. A 10  $\mu$ m scale bar is shown. The resolution improvement is a factor of about 6.

0.14  $\mu$ m. The NA increase also allows for the use of a smaller NA microscope objective lens without sacrificing the spatial resolution of the NAIL microscope. A microscope objective lens with NA=0.3 is sufficient to achieve the highest spatial resolution for a Si NAIL microscope. In Fig. 2, sub-surface inspection of a Si IC<sup>7</sup> using a Hamamatsu  $\mu$ AMOS-200, IC Failure Analysis System,<sup>5</sup> qualitatively displays the significant improvement provided by the NAIL. We show the image obtained using a 100 $\times$  microscope objective lens having NA=0.5 in Fig. 2(a), compared with that obtained using a 20 $\times$  microscope objective lens with a NAIL having NA=3.3 in Fig. 2(b). Features otherwise not visible can be clearly discerned using the NAIL technique.

For quantitative analysis of the lateral spatial resolution capability of the NAIL microscopy technique we imaged the same Si IC<sup>7</sup> using the confocal scanning optical microscope illustrated in Fig. 3. The specific NAIL we used has  $R=1.6$  mm and  $D=1.5$  mm, optimized for a substrate polished to a thickness of 500  $\mu$ m. The microscope objective lens has NA=0.3 resulting in the NAIL microscope having NA=3.4. Though a stigmatic image can also be obtained by means of a focal plane array, we scan the sample and NAIL with a 25  $\mu$ m pinhole placed in the image space. Note that the lateral precision of the mechanical scan is relaxed by a

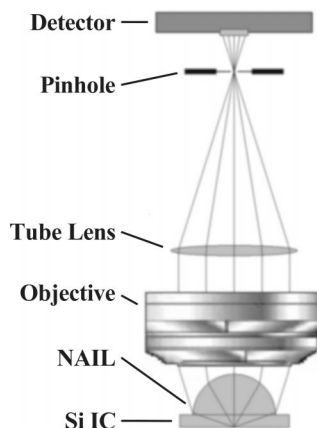


FIG. 3. NAIL confocal microscope configuration, where the Si IC and NAIL are scanned.

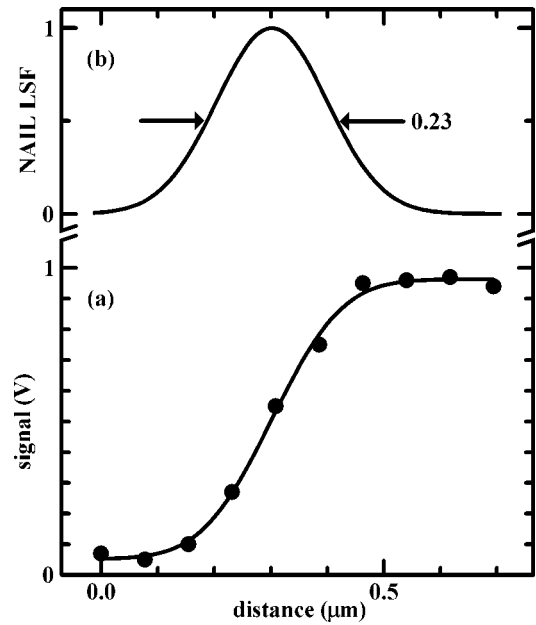


FIG. 4. Line scan across a physical edge with (a) fitted detector signal and (b) NAIL microscope line spread function (LSF) plotted by distance, demonstrating 0.23  $\mu$ m lateral spatial resolution by the Houston criterion.

factor of  $n^2$ , so a lateral 200  $\mu$ m mechanical movement of the sample and NAIL results in a lateral 15  $\mu$ m movement of the focal point in the object space. The longitudinal or vertical precision of the mechanical scan is relaxed by an even greater factor of  $n^3$ . A 1.05  $\mu$ m laser diode provides transmitted darkfield illumination to the sample and a cooled germanium detector offers a high detectivity.

We use an edge response to evaluate the lateral spatial resolution of the NAIL microscope. Taking a line scan across a physical edge, we obtain the error function fitted detector signal shown in Fig. 4(a). The edge response represents a convolution of the NAIL microscope line spread function and the physical edge structure. Assuming the physical edge to be a step function, we deconvolve the line spread function of the NAIL microscope shown in Fig. 4(b). The line spread function FWHM=0.23  $\mu$ m is the lateral spatial resolution of the NAIL microscope. Since the 0.18  $\mu$ m fabrication process of the Si IC<sup>7</sup> has a finite physical edge width, the actual lateral spatial resolution of the NAIL microscope is better than the measured 0.23  $\mu$ m. We also show in Fig. 5, a line

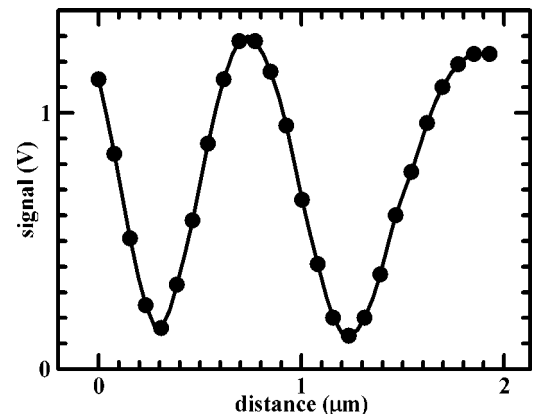


FIG. 5. Line scan across two closely separated features with the detector signal plotted by distance.

scan across two closely separated features. The two signal minima are separated by  $0.9 \mu\text{m}$  and demonstrate high contrast.

In conclusion, the NAIL subsurface microscopy technique we describe significantly increases the NA without introducing an additional spherical aberration. Consequently, the spatial resolution is improved beyond the limit of standard subsurface microscopy. Using the NAIL technique in the near infrared inspection of a Si IC,<sup>7</sup> the theoretical lateral spatial resolution limit is improved to  $0.14 \mu\text{m}$ . By realizing  $\text{NA}=3.4$  our experiments demonstrate a lateral spatial resolution of better than  $0.23 \mu\text{m}$ . Addition of the NAIL to a standard microscope also dramatically improves the longitudinal or vertical spatial resolution and we are currently developing a sample to verify this enhancement. The theoretical longitudinal spatial resolution limit is improved to

$0.08 \mu\text{m}$ , and we expect an experimental value with our NAIL microscope of better than  $0.13 \mu\text{m}$ .

The authors would like to acknowledge JDS Uniphase for providing the laser diode, and the DARPA HERETIC Program for supporting this project.

<sup>1</sup>S. M. Mansfield and G. S. Kino, Appl. Phys. Lett. **57**, 2615 (1990).

<sup>2</sup>B. D. Terris, H. J. Mamin, D. Rugar, W. R. Studenmund, and G. S. Kino, Appl. Phys. Lett. **65**, 388 (1994).

<sup>3</sup>K. Karrai, X. Lorenz, and L. Novotny, Appl. Phys. Lett. **77**, 3459 (2000).

<sup>4</sup>Q. Wu, G. D. Feke, and R. D. Grober, Appl. Phys. Lett. **75**, 4064 (1999).

<sup>5</sup>Instruments of Hamamatsu Corporation, 360 Foothill Road, Bridgewater, NJ 08807, <http://www.hamamatsu.com>

<sup>6</sup>M. Born and E. Wolf, *Principles of Optics*, 7th ed. (Cambridge University Press, New York, 1999), pp. 465 and 159.

<sup>7</sup>SRAM chip fabricated by a  $0.18 \mu\text{m}$  process from a major semiconductor manufacturer.